

Specific Expression of E-Tmod (Tmod1) in Horizontal Cells: Implications in Neuronal Cell Mechanics and Glaucomatous Retina

Weijuan Yao* and Lanping Amy Sung†

Abstract: Erythrocyte tropomodulin (E-Tmod) is a tropomyosin-binding and actin capping protein at the point end of the filaments. It is part of a molecular ruler that plays an important role in generating short actin protofilaments critical for the integrity of the cell membrane. Here, with the use of *E-Tmod+lacZ* mice, we demonstrated a specific E-Tmod expression in horizontal cells (HCs) in the retina, and analyzed the stress-strain relationship of HCs, vertically oriented neurons, and retinal ganglial cells (RGC) under normal and high intraocular pressure (IOP). Since their dendrites are oriented laterally in a plane and form most complicated synapses with multiple cone photoreceptors, HCs are subjected to a greater stress and strain than vertically oriented neurons. The specific E-Tmod expression suggests its role in protecting HCs from mechanical damages in certain eye diseases, such as glaucoma, a neurodegenerative disease of the retina characterized by an elevated IOP. A stress-strain analysis on axons of RGC that run horizontally but only anchor at the optical nerve head suggests that they may also be subjected to a higher mechanical stress, which leads to an increase in “cup-to-disc” ratio in a higher IOP or in glaucoma patients.

Keyword: erythrocyte tropomodulin, horizontal cells, retina, glaucoma

1 Introduction

Erythrocyte tropomodulin (E-Tmod or Tmod 1) is a tropomyosin (TM)-binding and actin-capping

protein first isolated from human erythrocytes (Fowler, 1987) that may play an important role in maintaining the integrity of the cell membrane (Chu *et al.*, 2003; Sung and Vera, 2003). cDNA cloning revealed that human E-Tmod is a 40.6-kDa protein (Sung *et al.*, 1992) encoded by a gene composed of 9 coding exons (Chu *et al.*, 2000). Human and mouse E-Tmod share a 95% homology in protein sequences and identical exon organization. It is transcribed from a downstream promoter (P_{E1}) 5' to exon 1 (E1), or an upstream promoter (P_{E0}) 5' to an untranslated exon E0 (Chu *et al.*, 2000). E-Tmod caps the slow-growing end (pointed end) of TM-coated actin filaments (Fowler *et al.*, 1993; Gregorio *et al.*, 1995) by binding to the N-terminus of TM (Sung and Lin, 1994; Vera *et al.*, 2000) and decreases the rate of actin de-polymerization (Weber *et al.*, 1994; Weber *et al.*, 1996).

In erythrocytes, E-Tmod binds to N-terminal end of the rod-like TM5 or TM5b (Sung *et al.*, 2000) and forms a molecular “T” ruler to define the length of actin protofilaments ~ 37 nm (Fig. 1) (Sung and Vera, 2003; Vera *et al.*, 2005). The actin protofilaments further dictate the number of spectrin dimers in the junctional complex (JC) and thus the topology of the membrane network – “spoked” hexagon. Such organization provides the elastic deformability of erythrocytes (Vera, *et al.*, 2005) and supports the mechanical stability of the lipid bilayer (Zhu *et al.*, 2007). Even though only the membrane skeleton in erythrocytes has been revealed by transmission electron microscopy, similar organization may exist in other cells, as homologs of membrane skeletal proteins have been detected in several non-erythroid cell membranes (Woo and Fowler, 1994; Almenar-Queralt *et al.*, 1999).

* Department of Bioengineering, University of California, San Diego La Jolla, CA 92093-0412

† Corresponding author. Department of Bioengineering, And Center for Molecular Genetics, University of California, San Diego. Tel: (858) 534-5250, Email: amy-sung@bioeng.ucsd.edu

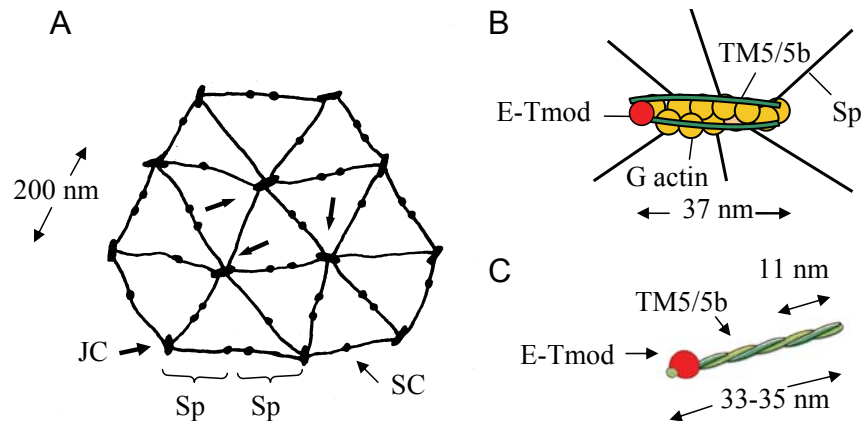


Figure 1: Schematic drawings of the hexagonal network in the erythrocyte membrane skeleton (A), a junctional complex (B), and an E-Tmod/TM complex (C) (modified from Sung and Vera, 2003) (A) An expanded hexagonal network, based on electron micrographs of erythrocytes in hypotonic solution; (B) A protofilament of ~ 37 nm associated two TM, an E-Tmod and six Sp; and (C) shows an E-Tmod/TM complex as a molecular ruler for the protofilament. JC, junctional complex; SC, suspension complex; and TM5/5b, tropomyosin isoform 5 and 5b homo- or heterodimer.

An exon 1 knockout (KO) and *lacZ* knock-in (KI) *E-Tmod* mouse model has been established in our lab (Chu *et al.*, 2003) followed by an exon 2 KO/KI model in other labs (Fritz-Six *et al.*, 2003). *E-Tmod* is highly expressed in several types of terminally differentiated cells, in which actin filament organization is critical for cell functions. These cells include erythrocytes, cardiomyocytes, skeletal muscle cells, lens fiber cells, and neurons in brain (Fowler, 1990; Sussman *et al.*, 1994; Woo and Fowler, 1994; Almenar-Queralt *et al.*, 1999; Yao *et al.*, 2007). The *E-Tmod* null mutation results in mechanical weakness of erythroid cells during deformation as determined by micropipette aspiration technique (Chu *et al.*, 2003). We took advantage of our *E-Tmod* KO mouse model that also has a *lacZ* gene knocked in downstream from the P_{E1} promoter to study the expression pattern of E-Tmod in the retina. The retina is a layered structure consisting of several kinds of neural cells that line the back of the eye. As shown in Fig. 2A, there are three layers of nerve cell bodies and two layers of synapses (Fu *et al.*, 2006). The outer nuclear layer (ONL) contains cell bodies of photoreceptor cells (cones and rods). The inner nuclear layer (INL) contains cell bodies of the horizontal, bipolar, and amacrine cells. The inner most layer is the ganglion cell

layer (GCL) that contains cell bodies of ganglion cells and some displaced amacrine cells. Dividing these nerve cell bodies are the two plexiform layers (*i.e.*, outer and inner plexiforms) where synaptic contacts occur. Between the retina and the sclera is the choroid coat, the vascular layer, with a thickness about 0.5 mm. On the other side, the retina is separated from the inside vitreous humour by the basal lamina.

In the retina, the axons and dendrites of most neurons, including photoreceptor cells and bipolar cells are parallel to the direction of light (or the axis of eyeball). Horizontal cells are major exceptions. Horizontal cells have laterally oriented dendrites and stratify within a very thin outer plexiform layer (OPL), where they make contact with the pedicles of cone photoreceptors. Structurally, the dendrites of adjacent horizontal cells overlap one another, so that multiple horizontal cells converge upon individual pedicles, the most complex synapses in the central neural system (CNS). Functionally, horizontal cells at OPL play an important role in integrating and modifying photoreceptor signals: when photoreceptor hyperpolarizes and reduces glutamate release as light is shined on it, horizontal cells reduce the release of gamma-aminobutyric acid (GABA), leading to the depolarization of photoreceptors (Yang *et al.*,

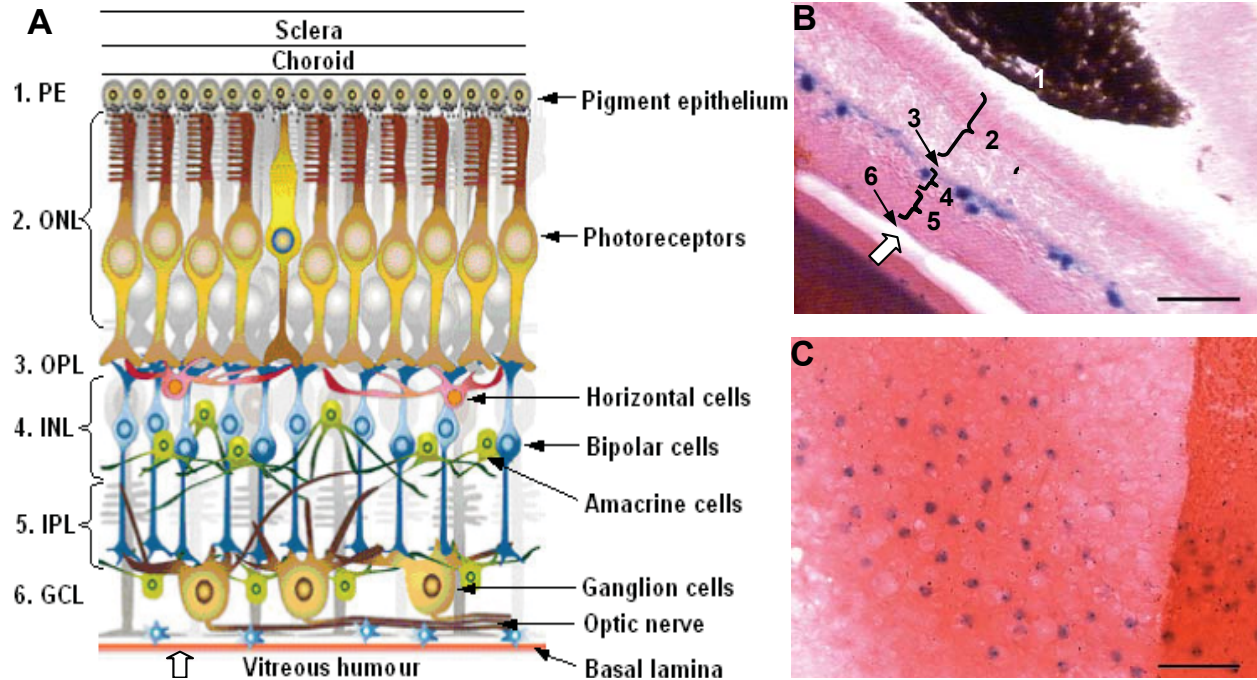


Figure 2: Layered organization of mouse retina and its expression pattern of E-Tmod. In retina (A) (modified from Fu *et al.*, 2006), pigmented epithelium (PE) is at the outer most layer (1); Rod and cone photoreceptor cells are within the outer nuclear layer (ONL, 2); Intermediate neurons, such as horizontal cells, bipolar cells, and amacrine cells are within the inner nuclear layer (INL, 4). Retinal ganglion cells are within the ganglion cell layer (GCL, 6), whose axons form optic nerve. OPL (3) and IPL (5) are outer plexiform and inner plexiform layers, respectively. The choroid and sclera layer, which are outside of the retina, and the vitreous humour, which is separated from retina by the basal lamina, are also labeled. In (B) and (C), the expression pattern of E-Tmod in an *E-Tmod* KO/KI mouse retina was revealed by X-gal staining. The transverse section (B) shows the *lacZ* positive horizontal cells at OPL, and a mosaic pattern in whole mount retina (C). The layers labeled in (B) are the same as in (A); the view direction in (C) is indicated (hollow arrows) in (A) and (B). Bars = 80 μ m.

1999).

The retina can be regarded as an elastic membrane or sheet, which stretches and deforms when a force is applied to it. The bovine retina has a Young's modulus of about 0.02 MPa or 20 kPa (Jones *et al.*, 1992). It is known that there is a circadian (24-hour) rhythm of intraocular pressure (IOP) in normal eyes (Liu, 1998). The change of daytime and nighttime IOP may therefore render the retina to different levels of stress. Furthermore, glaucoma, a neurodegenerative disease of the retina, is highly associated with elevated IOP. As a leading cause of irreversible vision loss worldwide, it is characterized by progressive retinal ganglion cell death (Gupta and Yücel, 2007). Indeed, in most glaucoma, an elevated IOP is a

major risk factor.

It is generally accepted that vision loss and dysfunction in elevated IOP induced glaucoma result from a progressive death, atrophy, and axon degeneration of retinal ganglion cells (RGCs), whose axons extend to central visual targets in the brain (Quigley and Green, 1979; Gupta and Yücel, 2007). No other neurons in the retina were visibly affected in glaucoma (Kendell *et al.*, 1995; Jakobs *et al.*, 2005). The nerve fibres from the retina leave the eye through pores in the lamina cribrosa (LC), which is a sieve-like structure in the optic nerve head (Morgan *et al.*, 1998), forming the optic disc. Blood vessels enter and leave the eye through the same structure. The nerve fibres form a rim around the edge of the optic nerve

head (neuro-retinal rim), leaving a central indentation without nerve fibres known as the optic cup. A cup-to-disc ratio over 0.5 increases the likelihood of glaucoma (Danesh-Meyer *et al.*, 2006).

It is important to understand the stress-strain relationship of soft tissues (Fung, 1993). In this study, different neurons in the retina are analyzed since the retina may be subjected to mechanical stress, such as IOP. Our recent studies by X-gal staining and immunofluorescent staining revealed that among all cell types in the retina, only horizontal cells express a high level of E-Tmod. This finding prompted us to model the biomechanics of horizontal cells, vertically oriented neurons, and axons of RGCs in healthy and glaucomatous retinas. Here we propose that some neuronal cells in the retina may undergo more remarkable deformation than others in normal physiology and certain diseases, depending on their orientations and their connections with neighbors. Our result suggests that horizontal cells may undergo more mechanical stress and strain (deformation) than other neurons in the retina, and that highly expressed E-Tmod in the horizontal cells may potentially have a protective role in maintaining the integrity of the cell membrane under stress.

2 Materials and Methods

Preparation of the retina sections. The eyes were isolated from adult *E-Tmod*^{+/-} mice and fixed in cold 4% paraformaldehyde and cryoprotected in 30% sucrose with 2 mM MgCl₂ at 4°C before embedded in Optimal Cutting Temperature (OCT) compound (Sakura Tissue Tek, Torrance, CA). Twelve- μ m frozen sections were cut on a cryostat (Leica, Germany).

X-gal staining. X-gal staining was performed following the protocol of Hogen (1986). Briefly, the sections on slides were post-fixed in 0.1 M phosphate buffer (PB, pH = 7.3) containing 0.2% glutaraldehyde. The slides were washed twice in PBS and transferred to detergent rinse (2 mM MgCl₂, 0.01% sodium deoxycholate, 0.02% NP-40 in PB) and then incubated in X-gal staining solution (detergent rinse solution supplemented with 5 mM potassium ferricyanide, 5 mM potassium ferrocyanide, and 1 mg/ml X-gal) at 37°C

for 1-3 hours in the dark. The slides were dehydrated and counterstained with 1% eosin. Bright field images were taken from an Olympus microscope.

3 Results

3.1 Specific expression of E-Tmod in horizontal cells

The knocked-in *lacZ* reporter gene in our *E-Tmod* knockout mouse model is under the control of endogenous P_{E1} promoter (Chu *et al.*, 2003). X-gal, a substrate of β -galactosidase (β -gal, *lacZ* gene product), can be converted to blue precipitates to signal where E-Tmod is normally expressed. The mouse retina was sectioned and followed by X-gal staining. The horizontal cells are found to be the only major cell type in the retina that specifically expresses *lacZ*. They align themselves into one layer in the transverse section of the retina (Fig. 2B) and show mosaic pattern in the whole mount retina (Fig. 2C). The density of the horizontal cells in this field is about 700 per mm². Immunohistochemistry has shown that E-Tmod is localized in the dendrites of horizontal cells, especially concentrated in the pedicle area (Yao and Sung, in preparation).

3.2 IOP and stress

IOP is determined by the equilibration between the aqueous humour production and the aqueous outflow. The pressure and volume relation for human eyes has been modeled (Friedenwald, 1937; Silver and Geyer, 2000). The elevated IOP may increase the intraocular volume of the eyeball (Fig. 3A) and generate circumferential stresses on the tissues surrounding the eyeball (Fig. 3E), including the retina.

If we consider the retina as a thin-walled sphere, the stress on the retina can be calculated using Eq. 1 (Higdon, 1985):

$$\sigma = P \cdot \frac{r}{2h} \quad (1)$$

where σ is stress (kPa); P is IOP (mmHg); r is the radius of the eyeball (12.5 mm) (Zinn and

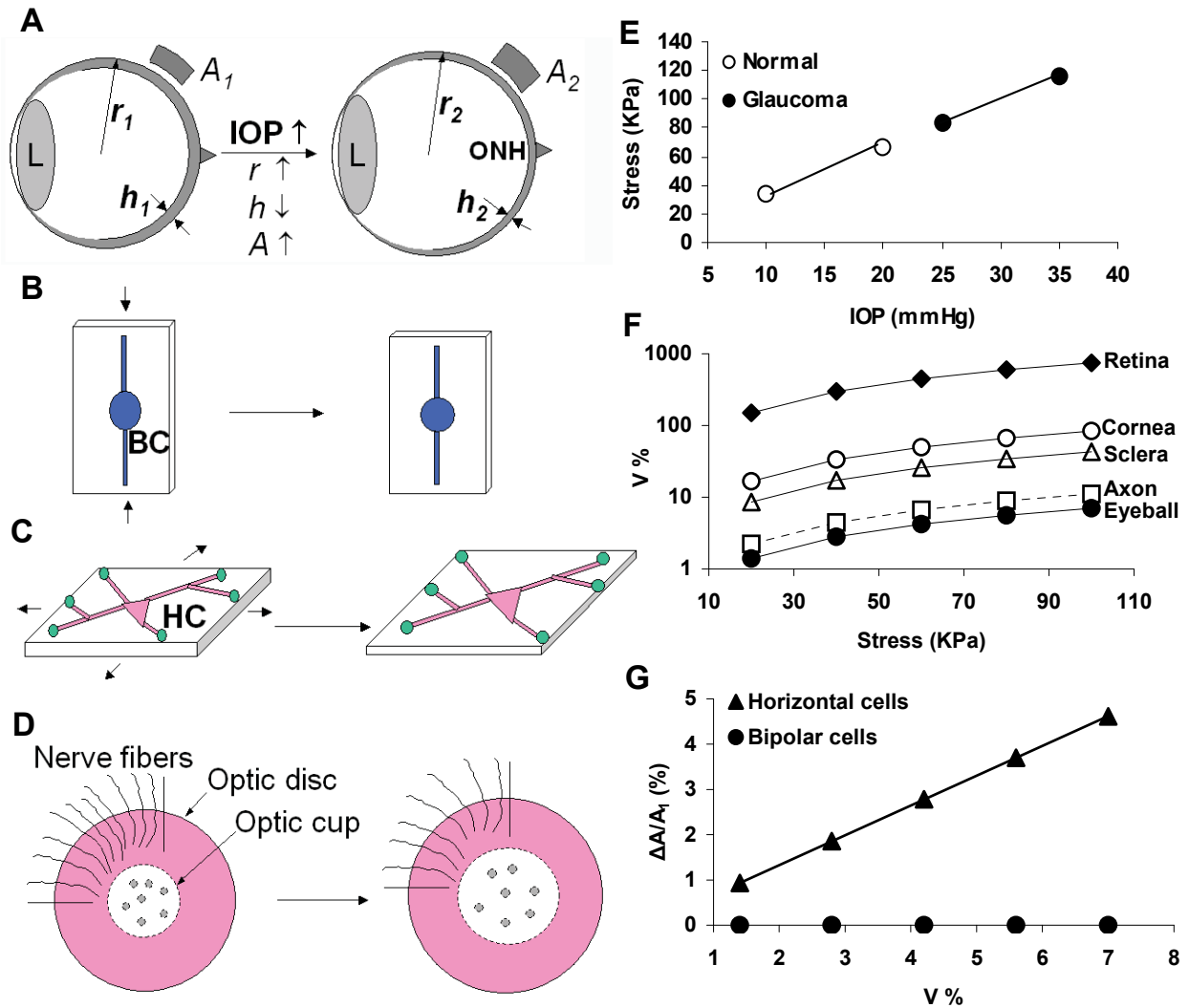


Figure 3: The stress-strain of horizontal cells and bipolar cells in retina as a function of intraocular pressure (IOP). (A) shows the volume change of eyeball in response to increase of IOP, resulting in the increase of radius (r), the decrease of thickness (h), and the surface area (A) of retina (grey). L , lens; ONH , optic nerve head. In (B), bipolar cells (BC), whose axon and dendrite parallel to the radius, undergo uniaxial deformation. In (C), horizontal cells (HC) with a wide spread dendritic field perpendicular to radius undergo equibiaxial deformation. The ends of dendrites are drawn as a circular area, emphasizing the connection with pedicles of photoreceptors and the expression of E-Tmod in this area. In (D), optic nerve head with optic nerve fibers, disc and cup and pores in lamina cribrosa (LC) are labeled. (E) shows the stress on the retinas under normal IOP range (10-20 mmHg) and glaucomatous range (25-35 mmHg). (F) shows the stress-strain ($\sigma - \epsilon$) relationship of retina, cornea, sclera, and eyeball. The strains are volumetric strain (V%) except for the axon (dashed line) which is a linear strain. In (G), ratios of surface area change (ΔA) of HC and BC relative to their initial areas (A_1) are plotted against the volumetric strain of the eyeball.

Solomon, 1965); and h is the thickness of the human retina (average $249 \pm 22 \mu\text{m}$) (Alamouti and Funk, 2003).

In a recent report, the IOPs in normal subjects and early-diagnosed, untreated glaucoma patients during 24 hours have been measured. At daytime, their supine IOPs are 20.4 ± 0.4 and 23.1 ± 0.7 mmHg, respectively (Liu *et al.*, 2003). Here we use a range of 10-20 mmHg for normal human eyes and 25-35 mmHg for glaucoma in our analysis. The stress produced by IOP on the retina of glaucomatous eyes is higher than that of normal eyes (Fig. 3E). The retina of glaucoma patients would thus be subjected to higher levels of stresses than that in normal individuals.

The strain (deformation) of cells and tissues in response to a stress is a function of their mechanical properties. Furthermore, individual neurons in the retina may also undergo different degrees of strain due to their different orientations and how their axons and/or dendrites are connected to the neighboring cells/tissues. The following sections, therefore, deal with the stress-strain relationships of the eyeball, its components, and several types of neurons in the retina with different organization and orientations.

3.3 Stress and strain of an eyeball and its components

An eyeball can be considered as a sphere and its enclosing membrane is elastic (Clark, 1932). When the eyeball enlarges, its volumetric strain $\frac{\Delta V}{V}$ can be determined by Eq. 2 (Pierscoinek *et al.*, 2007).

$$\frac{\Delta V}{V} = \frac{3\sigma}{E}(1 - \nu) \quad (2)$$

where σ is the stress on the eyeball; E is the Young's modulus (3 MPa) (Table 1); and ν is Poisson's ratio (0.3 for the eyeball). The stress-strain relationship of the eyeball as a whole is plotted in Fig. 3F. At stress of 100 KPa, for example, the eyeball will have a 7% of volume increase.

We then consider the major components in the eyeball, *i.e.*, retina, cornea, and sclera. The Young's modulus of bovine retina is 0.02 MPa

(Table 1), which is significantly smaller than that of the eyeball. If the retina experiences a stress of 100 KPa without other constrains, its volumetric strain will be 750% according to Eq. 2 ($\nu = 0.5$) (Fig. 3F). Since it is not reasonable physiologically for the retina to have a strain greater than that of the eyeball, the maximum strain of the retina would be equal to that of the eyeball. All the subsequent analyses use the maximal 10% volume change as an example.

The elastic moduli of the cornea and sclera have also been estimated (Table 1): They are 0.07-0.29 MPa and 0.2-0.5 MPa, respectively. We used the average values of 0.18 MPa for the cornea and 0.35 MPa for the sclera and plotted their volumetric strain (V%) against the stress. It is clear that the eyeball has the smallest strain as compared to the 3 separate components listed above (Fig. 3F). The apparent Young's modulus for the basement membrane of the adult mouse retina was 4.07 MPa (Table 1) as measured by atomic force microscopy (AFM) (Candiell *et al.*, 2007).

3.4 Stress and strain of vertically oriented neurons

We then consider the response of different neurons in the retina. For vertically oriented neurons, including photoreceptor cells and bipolar cells, their cell bodies, axons, and dendrites are approximately aligned in the same direction as the radius of the eyeball. When the radius of the eyeball expands (*e.g.*, with an increased IOP in disease or by physical compression), the surface area (A) of the retina will increase whereas its thickness (h) will decrease (Fig. 3A). Neurons arranged in the vertical direction will thus be compressed in the direction of radius, but thicken in the perpendicular direction. Furthermore since these vertically oriented cells do not have lateral anchorage points with neighboring neurons, they may undergo constant area shear deformation (Fig. 3B). Thus, the stress acting on these cells will likely not result in membrane damages (Fig. 3G).

Table 1: The elastic moduli of components in the eye.

Tissues*	Elastic modulus (MPa)	References
Eyeball	3	Zhou <i>et al.</i> , 2005
Retina (bovine)	0.02	Jones <i>et al.</i> , 1992
Cornea	0.07-0.29	Pierscionek <i>et al.</i> , 2007
Sclera	0.2-0.5	Pierscionek <i>et al.</i> , 2007
Basement membrane of retina (mouse)	4.07	Candiell <i>et al.</i> , 2007
Nerve fibers (mouse)	0.1-1.5	Heradia <i>et al.</i> , 2007
Lamina cribrosa	0.14-0.38	Edwards and Good, 2001

* Human, unless specified.

3.5 Stress and strain of horizontally oriented cells

On the contrary, the dendrites of horizontal cells are distributed in a large field on OPL, a plane that is parallel to the eyeball surface. In rats, there are about 815 horizontal cells per mm^2 and each horizontal cell may cover about $1/815 \text{ mm}^2 = 1,200 \mu\text{m}^2$ (Chun *et al.*, 1999). Each horizontal cell's dendrites form synaptic contacts with several photoreceptors (can not break loose easily), so when the intraocular volume increases due to an elevated IOP, horizontal cells will have an equibiaxial expansion in the plane of OPL (Fig. 3C). Since the volume of the eyeball is $V = \frac{4}{3}\pi \cdot r^3$, if the eyeball expands ($\frac{\Delta V}{V}$) 10%, the radius ratio ($\frac{r_2}{r_1}$) will become 1.0328. Thus, the surface area (A) of horizontal cells or OPL will have an equibiaxial expansion of 6.56% based on Eq. 3.

$$\frac{\Delta A}{A_1} = \frac{4\pi \cdot r_2^2 - 4\pi \cdot r_1^2}{4\pi \cdot r_1^2} = \left(\frac{r_2}{r_1}\right)^2 - 1 = 0.0656 \quad (3)$$

where A is surface area, and the surface area change vs. volumetric strain is plotted in Fig. 3G. This analysis suggests that laterally oriented cells that have multiple anchorage points would undergo significantly higher strain in surface area change in response to the stress as compared to the vertically oriented cells (see above).

3.6 Stress and strain of RGCs

Interestingly, RGCs arrange their axons perpendicular to the radius of the eyeball but their dendrites in the same direction of the radius. Their

axons, therefore, will undergo circumferential extension when intraocular volume changes, but restricted by the anchorage in the optic nerve head (ONH). The elastic modulus of nerve fibers has been measured by AFM (Heradia *et al.*, 2007). While myelinated axons have elastic modulus of 0.1-1.5 MPa, demyelinated axons have slightly lower but similar modulus (Table 1). We thus use the average value of 0.9 MPa for the axons of RGCs. Their stress and strain relationship is plotted (dashed line in Fig. 3E) following Eq. 4:

$$\varepsilon = \sigma/E \quad (4)$$

where ε is the strain; σ is the stress; and E is elastic modulus. As we calculated in last section, if the eyeball expands 10% in volume, axons of RGCs will have a linear strain of 3.28% as the circumference increases. The increase of circumference is the same as the increase of the radius since $\frac{\Delta l}{l} = \frac{2\pi \cdot r_2 - 2\pi \cdot r_1}{2\pi \cdot r_1} = \frac{\Delta r}{r_1}$, where l is the circumference that equals to the length of the axon.

Anatomically, the ONH is the beginning of the optic nerve in the retina or where the axons of RGCs exit the eye to form the optic nerve. There are approximately 1.1 million nerve cells in each optic nerve. In glaucoma, the nerve fibers are usually damaged and the loss of these fibers results in the increase of cup-to-disc ratio. Lamina cribrosa (LC), which nerve fibers pass through and consists of a series of collagenous plates, has an elastic modulus of 0.14-0.38 MPa (Table 1). When IOP increases, LC, cup and disc are expected to increase their areas due to the equibiaxial extension of the local tissues (Fig. 3D). However, since nerve fibers are coming from the whole

retina in the back of the eye, and they all enter LC from all directions, the fibers may also pull LC in a radial fashion against the disc, thus increase the cup-to-disc ratio. The further the RGCs are located from the disc, the greater the stress their axons may generate. Therefore the stress-strain of LC may not be homogeneous. Some of the nerve fibers may be damaged by the resistance of deformation in the LC, considering that the mean pore size is $0.004 \pm 0.001 \text{ mm}^2$ (Jonas *et al.*, 1991) and single nerve fiber has a diameter of $1 \mu\text{m}$ (Jonas and Hayreh, 1999). This may be one of the reasons that glaucoma patients lose their peripheral visions.

It has been modeled that when IOP increases, the ONH is subjected simultaneously to various modes of strain, including compression, extension and shearing (Sigal *et al.*, 2007). Finite element modeling (Sigal *et al.*, 2004) showed that LC could have an averaged strain (fractional elongation) of 4-5.5%, which is considered biologically significant and capable of contributing to the development of glaucomatous optic neuropathy.

4 Discussion

In this study we found that horizontal cells are the major cell type in the retina that specifically expressed E-Tmod. We followed by analyzing the stress-strain relationship of the retina and reveals that compared with vertically oriented neurons, horizontal cells may undergo higher stress and strain. Horizontal cells, however, appear resistant to degenerative processes induced by a high IOP in the retina. A previous study has showed that the density of horizontal cells remained unchanged after ischemia reperfusion (in which IOP increased to 90-120 mmHg by perfusion for 1 hour) even though the thickness of the retina became progressively thinner (Chun *et al.*, 1999). Interestingly, the study by Janssen *et al.* 1996 revealed that the mean horizontal cell soma (cell body) size was significantly increased (26%) in the glaucomatous retina, while the dendritic field size was not affected. The increase in soma size is thought to be indicative of horizontal cell's hypertrophy responses to the elevated IOP. We interpret that such hypertrophic adaptation may help

reduce the cell surface area change induced by the volumetric increase. For example, if the cell size (diameter) increases by 26%, at 10% of volumetric expansion $\frac{\Delta V}{V}$, the surface expansion $\frac{\Delta A}{A}$ will be reduced by 37% from 6.56% to 4.13%. This may help minimizes their membrane damages in horizontal cells.

It is known that erythrocytes with a flexible membrane skeleton, governed by E-Tmod and its associated proteins (Sung and Vera, 2003), are able to maintain the membrane integrity during cell deformation in circulation. Membrane skeletal protein, spectrin (240/235E), is present in the retina, especially concentrated in OPL (where horizontal cells are located) and IPL (Isayama *et al.*, 1991). Filamentous actin (F-actin) was found heavily distributed where horizontal cells make contacts (Vaughan and Lasater, 1990). The presence of TM isoforms in CNS has also been reported (Schevzov *et al.*, 1997; Vrhovski *et al.*, 2003). The presence of E-Tmod and its associated proteins (or their isoforms) may allow some neurons to form a membrane skeletal network similar to that in erythrocytes (see Fig. 1). Such similar structure if exists may protect the horizontal cell membranes from being damaged when they undergo mild daily deformations in normal physiology and larger deformations in certain diseases, *e.g.*, glaucoma.

Laterally oriented axons of RGCs may also be subjected to a higher stress, but their anchorage pattern is different from that of the horizontal cells. They do not express detectable level of E-Tmod, and show distinct sensitivities to mechanical stress. In glaucoma patients the damages may be resulted from the elongation of axons and the resistance by LC at ONH (reflected by an increase of the cup-to-disc ratio), leading to axon degeneration, optic nerve loss, and apoptosis of RGCs. There are, however, other studies indicate that RGCs can also be directly affected by the elevated IOP alone in glaucomatous retina. Agar and colleagues (2006) found that apoptosis is increased in cultured RGCs subjected to hydrostatic pressures mimicking conditions in acute (100 mmHg) and chronic (30 mmHg) glaucoma. Liu *et al.* (2007) demonstrated that oxida-

tive stress is an early event in hydrostatic pressure induced RGC damage. Furthermore, elevated hydrostatic pressure can trigger mitochondrial fission and decrease cellular ATP in differentiated RGC-5 cells (28).

It is worth noting that dendrites of amacrine cells are also oriented on a plane (IPL) parallel to the eyeball surface. The functions of amacrine cells are not fully understood. There are many types of amacrine cells and they differ greatly in size. Some have processes extending less than 100 μm but some have processes spreading 1,000 μm or more (for review, see Oyster, (34)). Depending on the cell types, dendrites are either laterally oriented (*e.g.*, starburst) or vertically oriented (*e.g.*, AII) within IPL, which is 35 μm thick, much thicker than OPL (12 μm) in C57Bl/6J mice (38) (see Fig. 2A). They receive signal inputs from rod photoreceptors and form synapses with bipolar cells and RGCs. Thus the interactions mediated by amacrine cells can be made over short and long distances, which modify the information flow and adjust the sensitivity of information transmission (34). The level of E-Tmod expression in the retina may be critically linked to stress and strain, which may be determined by the mechanical properties of the cells, the orientation of dendrites/axons and how they are connected with other neighboring neurons or tissues. The finding that the expression of E-Tmod by the *lacZ* reporter gene is not detectable in amacrine cells suggests they may experience a lower level of stress than that of horizontal cells, which is in agreement with that no change has been reported for amacrine cells in the studies of higher IOP or in glaucoma patients.

Acknowledgement: The study on E-Tmod was supported by NIH grant P01 HL043026-150001. We thank Dr. Robert Sah for the use of cryostat and Drs. John H. K. Liu, Gabe Silva, and Geert Schmid-Schönbein for helpful discussion.

References

1. Agar, A., Li, S., Agarwal, N., Coroneo, M.T., Hill, M.A. (2006) Retinal ganglion cell line

apoptosis induced by hydrostatic pressure. *Brain Res.* 1086, 191-200.

2. Alamouti, B., Funk, J. (2003) Retinal thickness decreases with age: an OCT study. *Br. J. Ophthalmol.* 87, 899-901.
3. Almenar-Queralt, A., Lee, A., Conley, C.A., Ribas de Pouplana, L., Fowler, V.M. (1999) Identification of a novel tropomodulin isoform, skeletal tropomodulin, that caps actin filament pointed ends in fast skeletal muscle. *J. Biol. Chem.* 274, 28466-28475.
4. Candiello, J., Balasubramani, M., Schreiber, E.M., Cole, G.J., Mayer, U., Halfter, W., Lin, H. (2007) Biomechanical properties of native basement membranes. *FEBS J.* 274, 2897-2908
5. Chu, X., Chen, J., Reedy, M.C., Vera, C., Sung, K.L., Sung, L.A. (2003) E-Tmod capping of actin filaments at the slow-growing end is required to establish mouse embryonic circulation. *Am. J. Physiol. Heart Circ. Physiol.* 284, H1827-1838.
6. Chu, X., Thompson, D., Yee, L.J., Sung, L.A. (2000) Genomic organization of mouse and human erythrocyte tropomodulin genes encoding the pointed end capping protein for the actin filaments. *Gene* 256, 271-281.
7. Chun, M., Kim, I., Ju, W., Kim, K., Lee, M., Joo, C., Chung, J. (1999) Horizontal cells of the rat retina are resistant to degenerative processes induced by ischemia-reperfusion. *Neurosci. Lett.* 260, 125-128.
8. Clark, J.H. (1932) A method for measuring elasticity in vivo and results obtained on the eyeball at different intraocular pressures. *Am. J. Physiol.* 101, 474-481.
9. Danesh-Meyer, H.V., Gaskin, B.J., Tayusundera, T., Donaldson, M., Gamble, G.D. (2006) Comparison of disc damage likelihood scale, cup to disc ratio, and Heidelberg retina tomograph in the diagnosis of glaucoma. *Br. J. Ophthalmol.* 90, 437-441.

10. Edwards, M.E, Good, T.A. (2001) Use of a mathematical model to estimate stress and strain during elevated pressure induced lamina cribrosa deformation. *Curr. Eye Res.* 23, 215–225.
11. Fowler, V.M. (1987) Identification and purification of a novel Mr 43,000 tropomyosin-binding protein from human erythrocyte membranes. *J. Biol. Chem.* 262, 12792-12800.
12. Fowler, V.M., Sussmann M.A., Miller P.G., Flucher, B.E., Daniels, M.P. (1993) Tropomodulin is associated with the free (pointed) ends of the thin filaments in rat skeletal muscle. *J. Cell Biol.* 120, 411-420.
13. Fritz-Six, K.L., Cox, P.R., Fischer, R.S., Xu, B., Gregorio, C.C., Zoghbi, H.Y., Fowler, V.M. (2003) Aberrant myofibril assembly in tropomodulin1 null mice leads to aborted heart development and embryonic lethality. *J. Cell Biol.* 163, 1033-1044.
14. Friedenwald, J.S. (1937) Contribution to the theory and practice of tonometry. *Am. J. Ophthalmol.* 20, 985-1024.
15. Fu, X., Sun, H., Klein, W.H., Mu, X. (2006) β -catenin is essential for lamination but not neurogenesis in mouse retinal development. *Dev. Biol.* 299, 424-437.
16. Fung, Y.C. (1993) *Biomechanics: mechanical properties of living tissues*. Second Edition. Springer-Verlag, New York.
17. Gregorio, C.C., Weber, A., Bondad, M., Pennise, C.R., Fowler, V.M. (1995) Requirement of pointed-end capping by tropomodulin to maintain actin filament length in embryonic chick cardiac myocytes. *Nature* 377, 83-86.
18. Gupta, N., Yücel, Y.H. (2007) Glaucoma as a neurodegenerative disease. *Curr. Opin. Ophthalmol.* 18,110-114.
19. Heredia, A., Bui, C.C., Suter, U., Young, P., Schäffer, T.E. (2007) AFM combines functional and morphological analysis of peripheral myelinated and demyelinated nerve fibers. *NeuroImage* 37, 1218-1226.
20. Higdon, A., Ohlsen, E.H., Stiles, W.B., Weese, J.A., Riley, W.F. (1985) *Mechanics of Materials*, Fourth Edition, John Wiley & Sons.
21. Hogan, B., Constantini, F., Lacy, E. (1986) *Manipulating the mouse, a laboratory manual*. Cold Spring Harbor. NY: Cold Spring Harbor Laboratory, 375.
22. Isayama, T., Goodman, S.R., Zagon, I.S. (1991). Spectrin isoforms in the mammalian retina. *J. Neurosci.* 11, 3531-3538.
23. Jakobs, T.C., Libby, R.T., Ben, Y., John, S.W., Masland, R.H. (2005) Retinal ganglion cell degeneration is topological but not cell type specific in DBA/2J mice. *J. Cell Biol.* 171, 313-325.
24. Janssen, P., Naskar, R., Moore, S., Thanos, S., Thiel, H.J. (1996) Evidence for glaucoma-induced horizontal cell alterations in the human retina. *Ger. J. Ophthalmol.* 5, 378-385.
25. Jonas, J.B., Hayreh, S.S. (1999) Localised retinal nerve fibre layer defects in chronic experimental high pressure glaucoma in rhesus monkeys. *Br. J. Ophthalmol.* 83, 1291-1295.
26. Jonas, J.B., Mardin, C.Y. Schlrörz-Schrehardr, U., Naumann, G.O.H. (1991) Morphometry of the human lamina cribrosa surface. *Invest. Ophthalmol. Vis. Sci.*, 32, 401-405.
27. Jones, I.L., Warner, M., Stevens, J.D. (1992) Mathematical modeling of the elastic properties of retina: A determination of Young's modulus. *Eye* 6, 556–559.
28. Ju, W.k., Liu, Q., Kim, K.Y., Crowston, J.G., Kindsy, J.D., Agarwal, N., Ellisman, M.H., Perkins, G.A., Weinreb, R.N. (2007) Elevated hydrostatic pressure triggers mitochondrial fission and decreases cellular ATP in differentiated RGC-5 cells. *Invest Ophthalmol Vis Sci* 48, 2145-2151.

29. Kendell, K.R., Quigley, H.A., Kerrigan, L.A., Pease, M.E., Quigley, E.N. (1995) Primary open-angle glaucoma is not associated with photoreceptor loss. *Invest. Ophthalmol. Vis. Sci.* 36, 200-205.
30. Liu, J.H.K. (1998). Circadian rhythm of intraocular pressure. *J. Glaucoma* 7, 141-147.
31. Liu, J.H.K., Zhang, X., Kripke, D.F., Weinreb, R.N. (2003) Twenty-four-hour intraocular pressure pattern associated with early glaucomatous changes. *Invest. Ophthalmol. Vis. Sci.* 44, 1586-1590.
32. Liu, Q., Ju, W.K., Crowston, J.G., Xie, F., Perry, G., Smith, M.A., Lindsey, J.D., Weinreb, R.N. (2007) Oxidative stress is an early event in hydrostatic pressure induced retinal ganglion cell damage. *Invest. Ophthalmol. Vis. Sci.* 48, 4580-4589.
33. Morgan, J.E., Jeffery, G., Foss, A.J.E. (1998) Axon deviation in the human lamina cribrosa. *Br. J. Ophthalmol.* 82, 680-683.
34. Oyster, C.W. (1999) *The human eye: structure and function*. 1st Edition, Sinauer, Sunderland, Massachusetts, pp. 595-631.
35. Pierscoinek, B.K., Asejczyk-Widlicka, M., Schachar, R.A. (2007) The effect of changing intraocular pressure on the corneal and scleral curvatures in the fresh porcine eye. *Br. J. Ophthalmol.* 91, 801-803.
36. Quigley, H.A., Green, W.R. (1979). The histology of human glaucoma cupping and optic nerve damage: clinicopathologic correlation in 21 eyes. *Ophthalmology* 10, 1803-1827.
37. Raven, M.A., Stagg, S.B., Nassar, H., Reese, B.E. (2005) Developmental improvement in the regularity and packing of mouse horizontal cells: implications for mechanisms underlying mosaic pattern formation. *Vis. Neurosci.* 22, 569-573.
38. Sano, Y., Furuta, A., Setsuie, R., Kikuchi, H., Wang, Y., Sakurai, M., Kwon, J., Noda, M., Wada, K. (2006) Photoreceptor Cell Apoptosis in the Retinal Degeneration of *Uchl3*-Deficient Mice. *Am. J. Pathol.* 169, 132-141.
39. Schevzov, G., Gunning, P., Jeffrey, P.L., Temm-Grove, C., Helfman, D.M., Lin, J.J., Weinberger, R.P., (1997) Tropomyosin localization reveals distinct population of microfilaments in neurites and growth cones. *Mol. Cell Neurosci.* 8, 439-454.
40. Sigal, I.A., Flanagan, J.G., Tertinegg, I., Ethier, C.R. (2004) Finite element modeling of optic nerve head biomechanics. *Invest Ophthalmol. Vis. Sci.* 45, 4378-4387.
41. Sigal, I.A., Flanagan, J.G., Tertinegg, I., Ethier, C.R. (2007) Predicted extension, compression and shearing of optic nerve head tissues. *Exp. Eye Res.* 85, 312-322.
42. Silver, D.M., Geyer, O. (2000) Pressure-volume relation for the living human eye. *Curr. Eye Res.* 20, 115-120.
43. Sung, L.A., Fowler, V.M., Lambert, K., Sussman, M.A., Karr, D., Chien, S. (1992) Molecular cloning and characterization of human fetal liver tropomodulin. A tropomyosin-binding protein. *J. Biol. Chem.* 267, 2616-2621.
44. Sung, L.A., Gao, K.M., Yee, L.J., Temm-Grove, C.J., Helfman, D.M., Lin, J.J., Mehrpouryan, M. (2000) Tropomyosin isoform 5b is expressed in human erythrocytes: implications of tropomodulin-TM5 or tropomodulin-TM5b complexes in the protofilament and hexagonal organization of membrane skeletons. *Blood* 95, 1473-1480.
45. Sung, L.A., Lin, J.J. (1994) Erythrocyte tropomodulin binds to the N-terminus of hTM5, a tropomyosin isoform encoded by the gamma-tropomyosin gene. *Biochemical and biophysical research communications* 201, 627-634.
46. Sung, LA, Vera, C. (2003) Protofilament and hexagon: a three-dimensional mechanical model for the junctional complex in the

- erythrocyte membrane skeleton. *Ann. Biomed. Eng.* 31, 1314-1326.
47. Sussman, M.A., Sakhi, S., Tocco, G., Najm, I., Baudry, M., Kedes, L., Schreiber, S.S. (1994) Neural tropomodulin: developmental expression and effect of seizure activity. *Brain Res. Dev. Brain Res.* 80, 45-53.
 48. Tan, J.C.H., Kalapesi F.B., Coroneo, M.T. (2006) Mechanosensitivity and the eye: cells coping with the pressure. *Br. J. Ophthalmol.* 90, 383-388.
 49. Vaughan, D.K., Lasater, E.M. (1990) Distribution of F-actin in bipolar and horizontal cells of bass retinas. *Am. J. Physiol. Cell Physiol.* 259, C205-C214.
 50. Vera, C., Lao, J., Hamelberg, D., Sung, L.A. (2005) Mapping the tropomyosin isoform 5 binding site on human erythrocyte tropomodulin: further insights into E-Tmod/TM5 interaction. *Arch. Biochem. Biophys.* 444, 130-138.
 51. Vera, C., Sood, A., Gao, K.M., Yee, L.J., Lin, J.J., Sung, L.A. (2000) Tropomodulin-Binding Site Mapped to Residues 7-14 at the N-Terminal Heptad Repeats of Tropomyosin Isoform 5. *Archives of Biochemistry and Biophysics* 378, 16-24.
 52. Vrhovski, B., Schevzov, G., Dingle, S., Lessard, J.L., Gunning, P., Weinberger, R.P. (2003) Tropomyosin isoforms from the gamma gene differing at the C-terminus are spatially and developmentally regulated in the brain. *J. Neurosci. Res.* 72, 373-383.
 53. Weber, A., Pennise, C.R., Babcock, G.G., Fowler, V.M. (1994) Tropomodulin caps the pointed ends of actin filaments. *J. Cell Biol.* 127, 1627-1635.
 54. Weber, A., Pennise, C.R., Fowler, V.M. (1999) Tropomodulin increases the critical concentration of barbed end-capped actin filaments by converting ADP. P(i)-actin to ADP-actin at all pointed filament ends. *J. Biol. Chem.* 274, 34637-34645.
 55. Woo, M.K., Fowler, V.M. (1994). Identification and characterization of tropomodulin and tropomyosin in the adult rat lens. *J. Cell Sci.* 107, 1359-1367.
 56. Yang, X., Gao, F., Wu, S.M. (1999) Modulation of horizontal cell function by GABAA and GABAC receptors in dark- and light-adapted tiger salamander retina. *Vis. Neurosci.* 16, 967-979.
 57. Yao, W., Nathanson, J., Lian, I., Gage, F.H., Sung, L.A. (2007) Mouse erythrocyte tropomodulin in the brain reported by lacZ knocked-in downstream from the E1 promoter. *Gene Expr. Patterns* 8, 36-46.
 58. Zhou, Y., Wang, G., Ding, H., Jiao, Y. (2005) Finite Element Modeling and Biomechanical Analysis of Eyeball and Extraocular Muscles. *Proc. 2005 IEEE.* 4978-4981.
 59. Zhu, Q., Vera, C., Asaro, R.J., Sche, P., Sung, L.A. (2007) A hybrid model for erythrocyte membrane: a single unit of protein network coupled with lipid bilayer. *Biophysical Journal* 93, 386-400.
 60. Zinn, W., Solomon, H. (1965) *Eye care, eye glasses and contact lenses.* City: Lifetime Books, 10.